Electronic transport in $Cs_2(TCNQ)_3$

J. S. Blakemore,* J. E. Lane,† and D. A. Woodbury‡
Department of Physics, Florida Atlantic University, Boca Raton, Florida 33431
(Received 17 March 1978)

Transport measurements are reported for $Cs_2(TCNQ)_3$ single crystals, conductivity from 100 to 500 K and thermopower from 200 to 400 K, both for the preferentially conducting $\vec{b}$ axis and for directions in the (010) plane. Results for $T > 300$ K indicate intrinsic behavior, with $\epsilon_i = (0.715 - 5 \times 10^{-4}T)$ eV, and with $\mu_n = 1.9\mu_p = 0.65$ cm^2/V sec for $\vec{b}$-axis conduction. At high temperatures, the thermopower is positive for direction $\vec{a}$, but negative for directions $\vec{b}$ and $\vec{c}^*$. Below room temperature, the thermopower becomes large and positive for all directions ($\Theta > +1000$ μV/K for $T < 250$ K), with significant intersample differences. The conductivity is similarly sample dependent below 300 K, with a slight reduction of activation energy. An analysis of $\vec{b}$-axis conduction and thermopower shows that this can be accounted for with a narrow-band model (using Fermi-Dirac one-electron statistics and one-dimensional density of states factors) with low-temperature behavior controlled by $\sim 10^{17}$ cm^{-3} of deep-level acceptors ($\epsilon_a = 0.303$ eV), and partial compensation that varies from sample to sample. Transport in directions normal to [010] is expected to have temperature dependences reflective of the statistics of the $\vec{b}$ axis, even though band motion is not valid in these directions.

I. INTRODUCTION

Conduction processes in organic solids have attracted considerable attention since the first reports of conduction in charge-transfer salts, particularly those of tetracyanoquinodimethane (TCNQ).[1,2] Much of that attention has been paid to highly anisotropic conduction in pseudo-one-dimensional solids, as reviewed for example by Shchegolev[3] and in recent books edited by Keller[4] and Wudl.[5] This has been greatly stimulated by research on tetrathiofulvalenium-tetracyanoquinodimethanide (TTF-TCNQ),[6,7] and its numerous derivative salts. The various phenomena which have been theoretically predicted for one-dimensional (1-D) metallic conduction (charge- and spin-density waves, 1D superconductivity, Peierls transitions, etc.) have produced many papers on the theoretical and experimental aspects of the metallic state, though the semiconducting salts of TCNQ have by no means been ignored during this period.[8]

TCNQ salts can be classified in a number of ways,[9] and one of the most important differences lies between those with segregated side-by-side donor and acceptor stacks and those with structures in which donors and acceptors alternate (as in an inorganic alkali halide). Stucky *et al.*[10] use the names *heterosoric* and *homosoric* for these two classes of structure, but the terms *segregated* and *alternating* have been widely used. Another significant distinction lies between *simple* salts with a 1:1 donor:acceptor ratio, and *complex* salts with m:n stoichiometry. The crystal must contain some formally neutral TCNQ if $n > m$, as is ordinarily the case for complex TCNQ salts, including $Cs_2(TCNQ)_3$.

An understanding of TCNQ salts with highly anisotropic quasimetallic conduction, phase transitions, and other complexities has of necessity required some rather sophisticated many-body theoretical concepts. However, it has been pointed out by Kommandeur[11] that many aspects of TCNQ salts are still amenable to interpretation by one-electron theory. It has thus been interesting to see a recent reinterpretation[12] of electronic conduction in NMP-TCNQ, which does not call for a phase transition, and which uses one-electron semiconductor statistics, modified only in the use of 1D density-of-states factors. The analysis of $Cs_2(TCNQ)_3$ in this paper follows the lines of one-electron theory, with the additional semiconductor supposition that substantial thermal ionization occurs from deep-lying localized impurity states.

Impurity effects have been invoked to explain some phenomena in organic solids, but not always in the same sense as in a conventional inorganic semiconductor. Thus, the lattice defects that must occur in any real crystal are taken into account in the interrupted strand model[13,14] of nearly-one-dimensional metallic conduction. This model, applied to triethylammonium-ditetracyanoquinodimethanide [TEA$(TCNQ)_2$] by Farges[15] and Brau[16] postulates metallic strands containing insulating defects, with hopping allowed sideways between strands. An advantage of this model is its ability to account for intersample variations of stacking-axis conductivity. However, since for $Cs_2(TCNQ)_3$ we find intersample differences of conductivity for low temperatures but not for higher ones, an extrinsic-intrinsic model seems more likely.

Impurities have sometimes been suggested as responsible for various aspects of thermopower behavior in organic solids. Buravov *et al.*[17] attributed the smallness of thermopower in quinolinium-TCNQ and acridinium-TCNQ crystals to impurity effects; also the thermopower data of Chaikin *et al.*[18] for TTF-TCNQ in the low-temperature semiconductor phase showed intersample differences suggestive of extrinsic effects.

We thus consider it significant that Eldridge[19] has observed both intrinsic and extrinsic photoconductivity for semiconducting TTF-TCNQ at $T = 5$ K, with a spectrum indicative of a deep-level impurity, having a binding energy some 30% of the intrinsic gap width. Shallower impurity levels appear to result from the doping of polyacetylene, for which Chiang *et al.*[20] have reported dramatic conductivity increases upon doping either n-type or p-type.

X-ray diffraction studies have shown[21-23] that the complex salt $Cs_2(TCNQ)_3$ has a monoclinic structure; the space group is P_21/c, and the unit-cell dimensions are $a = 7.34$ Å, $b = 10.40$ Å, $c = 21.98$ Å, $\beta = 97.8°$. The unique twofold $\vec{b}$-axis [010] is the direction along which the segregated Cs and TCNQ columns stack, and this is a naturally preferred growth direction.

The unit cell contains two formula units, which we should describe as four Cs^+ ions and two $TCNQ^0(TCNQ^-)_2$ trimers since x-ray diffraction[22,23] shows a trimeric modulation of TCNQ spacings along those stacks. The intermolecular spacing is 3.22 Å within a trimer, and 3.26 Å between trimers, and photoemission studies[24] find each neutral TCNQ sandwiched between a pair of $TCNQ^-$ ions. Torrance and Silverman noted[25] that stability of the segregated structure in this salt is preserved only by the inclusion of one-third neutral TCNQ's, ameliorating the consequences of electrostatic repulsion between like charges on the TCNQ stack.

The TCNQ stack structure is further complicated in that not all TCNQ's in a stack are parallel: the plane of each centric molecule (one at a center of symmetry) is tilted some 2° from that of the noncentric TCNQ's.[23] Whereas a centric molecule can be related to its nearest neighbors along the stack by the same overlap integral t on either side, a noncentric TCNQ is related to its centric neighbor by t but to its noncentric neighbor by $t' \neq t$, and is in a quite different environment. This variation of intermolecular interactions suggests a splitting of the unperturbed band owing to this periodic disturbance, and this is taken into account in band models.[26,27] A Hubbard-band 1D ($\vec{b}$-axis) tight binding band model for $Cs_2(TCNQ)_3$ developed by Soos and Klein[26] yields a three-band spectrum with Brillouin zone boundaries at $\pm\pi/3b$, the lowest band being filled.

The following sections sketch prior experimental work on the electrical and optical properties of $Cs_2(TCNQ)_3$ and illustrate results we have obtained for conductivity and thermopower in several groups of single crystals. These results, as indicated in in a preliminary report,[28] can be accounted for quite well by a fairly conventional semiconductor interpretation, modified in view of the anisotropy to a "pseudo-one-dimensional" band situation.

II. PREVIOUS EXPERIMENTAL WORK

Siemons *et al.*[2] measured the conductivity of both compaction samples and single crystals of $Cs_2(TCNQ)_3$ from room temperature down to 90 K. For the $\vec{b}$ axis in single crystals, they found $\sigma_b \simeq 10^{-3}$ Ω^{-1} cm^{-1} at room temperature, decreasing exponentially on cooling [$\sigma_b \simeq \sigma_0 \exp(-0.3/kT)$] down to $\sigma_b \simeq 10^{-16}\Omega^{-1}$ cm^{-1} at 90 K. This result has been interpreted as indicative of a 0.6-eV intrinsic gap, which is not inconsistent with the rather confusing data obtained by optical reflectivity and absorption methods.[29-31] The single crystal optical data of Hiroma *et al.*[30] have been interpreted by Torrance *et al.*[32] to signify an energy of ~0.6 eV for the charge transfer excitation of an electron from an occupied $TCNQ^-$ to a neighboring netural $TCNQ^0$, and of ~1.4 eV for transfer from $TCNQ^-$ to $TCNQ^-$.

For directions in the (010) plane, normal to the stacking direction, Siemons *et al.* found a conductivity with the same temperature dependence as in the favored direction, but some 25 times smaller. (Our own work puts this ratio closer to 50.) The superiority of [010] for conduction is entirely to be expected in view of the segregated stack structure, with its opportunity for relatively easy movement of electrons along the TCNQ stacks.

Siemons *et al.* also measured $\vec{b}$-axis thermopower, with results variable both in sign and magnitude from one sample to another. Their most reliable single-crystal thermopower data indicated a Seebeck coefficient of some -500 μV/K at room temperature, increasing to some -1000 μV/K on cooling to 200 K.

Sakai *et al.*[33] measured single-crystal $\vec{b}$-axis conductivity from room temperature to >500 K. Their room-temperature conductivity agreed with that of Siemons *et al.*,[2] and they found a similar activation energy up to about 400 K, but a substantially steeper slope for higher temperatures. They interpreted this as due to the competition of two intrinsic processes; transfers from $TCNQ^-$ to $TCNQ^0$ and from $TCNQ^-$ to $TCNQ^-$, with the 0.6- and 1.4-eV energies deducible from the optical

spectra of Hiroma *et al.*[30] Sakai *et al.* found that $Cs_2(TCNQ)_3$ starts to decompose around 500 K.

III. EXPERIMENTAL PROCEDURES

Crystals studied in our work were grown by the solution method of Melby *et al.*,[34] with metathesis of CsI and Li(TCNQ) in hot acetonitrile, which was then allowed to cool slowly. Deep-purple crystals resulted, with a shape typified by the idealized sketch of Fig. 1.

TCNQ was obtained commercially[35] and was purified before use by vacuum sublimation at 200 °C. A reaction described by Melby *et al.* was used to prepare Li(TCNQ), using lithium iodide.[36] Aldrich "Spectroquality" acetonitrile was used without further purification for the crystals reported on here; some preliminary preparations used other grades of acetonitrile that had been distilled from P_2O_5 before use. Elemental analyses for C, H, and N in intermediate and final products were indicative of stoichiometric TCNQ, though of course the sensitivity limit for this procedure is no better than 10^{18} cm^{-3}.

Precession and Laue film x-ray diffraction methods were used to confirm that our crystals had the structure and unit cell dimensions previously reported [21-23] for $Cs_2(TCNQ)_3$. As expected, the $\vec{b}$ axis was invariably the largest dimension of our crystals; typical sizes were 0.5–2 mm along [010] and some ten times smaller in the (010) plane. X-ray and optical methods were used to establish that the six prominent faces normal to (010) were members of the {001} and {102} families of crystal planes.[28]

Each preparative batch yielded numerous small crystals, of varying sizes but with morphology essentially as sketched in Fig. 1. This paper reports specifically on three groups of crystals, grown under slightly different condition. For simplicity in reporting, they are referred to herein as groups 1, 2, and 3,[37] though they were in fact successors to numerous earlier preparative batches, and the "working" system for numbering batches and of measured crystals from the various batches was much more complicated.

Group-1 crystals were grown from a solution containing a 50% molar excess of Cs, and group-2 crystals with a cation excess 50% larger again. In contrast, group-3 crystals grew from a solution with a 25% molar excess of TCNQ. The result in that case was a mass of intertwined purple $Cs_2(TCNQ)_3$ and yellow TCNQ crystals. Even so, individual purple crystals could be extracted for analysis or meausrement, and these crystals of group 3 were structurally and chemically "pure" $Cs_2(TCNQ)_3$. This exemplifies the thermodynamic preference for a crystal to experience self-cleaning while growing from a solution containing other solutes. Differences of properties between crystals of groups 1–3 were discernable only by semiconductor transport measurements. Those differences may or may not have stemmed from the deliberate distinctions of cation:anion ratio in the three solutions, for other (uncontrolled) factors

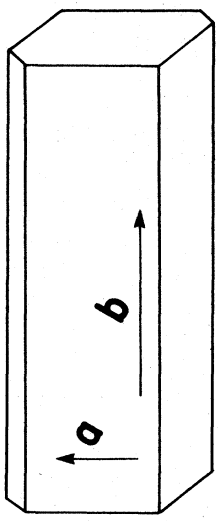

FIG. 1. Visual appearance (idealized) of a $Cs_2(TCNQ)_3$ crystal grown from acetonitrile solution, showing the directions $\vec{a}$ and $\vec{b}$ (the unique monoclinic axis). Measurements were made along $\vec{a}$, $\vec{b}$, and $\vec{c}^* = \vec{a} \times \vec{b}$.

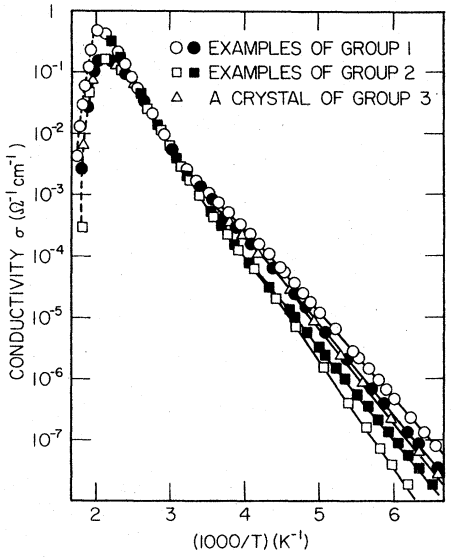

FIG. 2. Variation with $1/T$ of $\vec{b}$-axis conductivity for single crystals as examples of groups 1–3.

may well have been at work also. The electrical data (as exemplified by the $\vec{b}$-axis conductivity curves of Fig. 2) suggests that group-2 crystals were less tainted by extrinsic agents than those of the other two groups. Melby *et al.*[34] commented that the molar anion:cation ratio in the solvent might affect the "purity" of TCNQ salts, but there can clearly be other chemical influences also.

Identification of samples only by the number (1, 2, or 3) of the batch is proper only if intersample differences *within* a group are substantially smaller than those *between* groups. The samples chosen for Fig. 2 were selected to illustrate a "worst-case" situation, with an example of group 3 compared to two (extreme) examples each of groups 1 and 2. Extreme examples were selected here to show that, while crystals of a given group were not identical in their conductivity (or thermopower) behavior, these differences were not so large as to mask the evidence of differences among the three numbered groups. *All* crystals of group 2 conducted less well at low temperatures than *any* crystals of group 1, for example.

In some cases, it was possible to cut a long crystal into shorter sections for separate measurements in several directions. It was never possible to preserve exactly the same piece of a crystal for both conductivity and thermopower measurements—a contrast from the luxury of multiple measurements that can be made with a sturdy inorganic crystal.

As reported in a brief account of this work,[28] single crystal measurements of conductivity (σ) and thermopower (Θ) were made as functions of temperature for the directions $\vec{a}$, $\vec{b}$, and $\vec{c}^{\,*}=\vec{a}\times\vec{b}$. The latter is 7.8° away from $\vec{c}$, but is the natural choice for field alignment with the smallest crystal dimension. Van der Pauw conductivity measurements[38,39] were also made in the (010) plane; the quantity so found is the geometric mean of the principal components in that plane.[40] Contacts were made with DuPont No. 7941 silver paste for all measurements.

Chaikin and Kwak[41] have described a small ΔT technique for thermopower measurements, based on raising either end (face) of the crystal to successively higher temperatures while maintaining $\Delta T < 0.25$ K. This allows direct identification of stray emf's not due to ΔT, while displaying the temperature derivative of the voltage as the slope on a recorder trace. For our study, a small gradient apparatus was designed so that the sample and its environment were adjusted to a temperature of interest either by cooling with a CryoTip Joule-Kelvin refrigerator or with an electrical heater. A second heat source then raised one face a degree or two above the other, with a Cu-constantan thermocouple embedded in the contact material of each face. Measurements of the Seebeck voltage were made as a function of ΔT to check for stray emf's, and if necessary the true $\Delta V/\Delta T$ was obtained from a combination of such measurements. This approach afforded the larger signals desirable for study of a high impedance material such as $Cs_2(TCNQ)_3$. In view of the fragility of the crystals, and the need for thermopower measurements during the course of repeated cooling and heating cycles, it was necessary to arrange the thermal and electrical connections with considerable delicacy (heat sink electrically isolated with G. E. No. 7031 cement, strain-relieving wire connection to the warm face, etc.) to minimize the strain on a sample under measurement.

Conductivity measurements above 400 K were made to the point of materials failure, signalled by a rapid and irreversible fall of the conductance. The temperature for the conductance maximum was found to be around 500 K, as noted by Sakai *et al.*,[33] but was dependent on how long each measurement temperature was maintained; the faster the measurements, the higher one could hope to get. This precluded thermopower measurements above 400 K, since such observations just could not be taken fast enough to keep the crystal intact! A lower limit for thermopower data of just over 200 K was dictated by the variability of the Seebeck voltage (as measured with an electrometer) for sample resistances exceeding 10^{11} Ω.

IV. RESULTS

Figure 2 shows the general form of temperature dependence for $\vec{b}$-axis conductivity for samples from groups 1–3. The rather spectacular collapse of conductivity resulting from an excessive combination of time and high temperature is seen at the left, but will not be referred to again. Our principal concern in Fig. 2 is that all samples have essentially the same conductivity behavior for room temperature and above (within the limits that the geometric conversion from measured conductance to deduced conductivity can be made), whereas non-negligible differences do occur for lower temperatures. As mentioned in Sec. III, extreme examples were selected for this figure to show that crystals from within a numbered group are *not* identical, but from this point on we shall concentrate on the appreciably larger differences *between* groups. Thus numbering for Figs. 3–7 identifies only group number, and direction (labeled *A*, *B*, or *C**) of the conductivity or thermopower measurement.

From just below 300 to about 450 K, all samples have the same activated behavior, with a slope

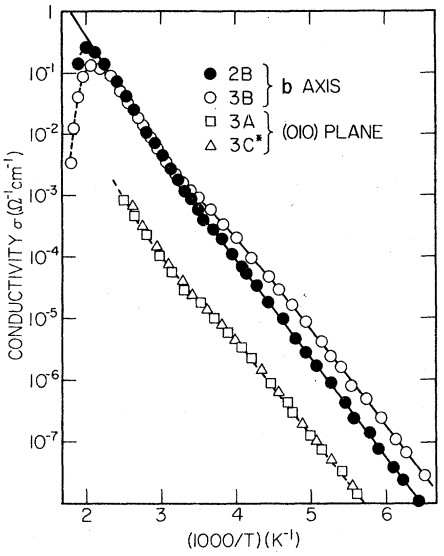

FIG. 3. Conductivity along the three orthogonal directions for typical crystals of group 3, compared with $\vec{b}$-axis conductivity for a typical group-2 crystal. The lines joining data points for the two $\vec{b}$-axis examples are computed from the numerical model, with parameters of Table I.

comparable to that of Sakai *et al.*[33] or from an extrapolation of the data of Siemons *et al.*[2] to higher temperatures. However, σ is significantly sample dependent (especially preparative-group dependent) for lower temperatures, a fact noted during the study of preliminary samples from the earlier preparative groups of crystals. Conductivity and

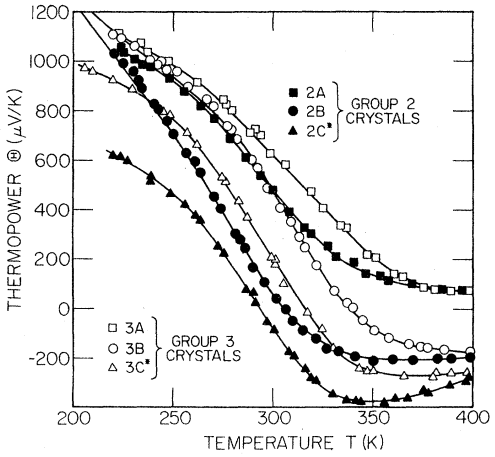

FIG. 4. Thermopower vs T for typical crystals of groups 2 and 3, as measured for the three orthogonal directions. The lines for $\vec{b}$-axis samples are computed from the numerical model, with parameters of Table I.

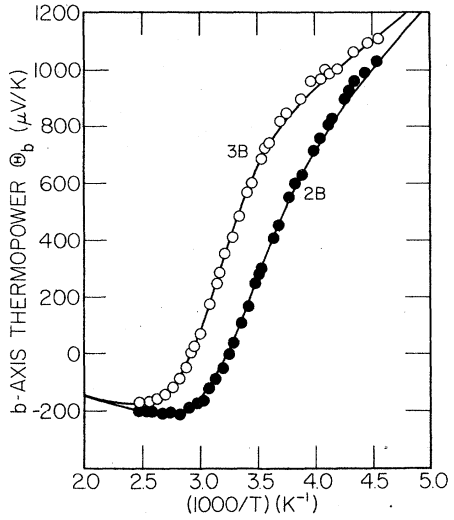

FIG. 5. Thermopower plotted vs $1/T$ for the $\vec{b}$ direction, data for the same two $\vec{b}$-axis samples as in Fig. 3, and with similarly calculated curves.

thermopower samples from groups 2 and 3 were selected for a detailed numerical analysis of what "impurity" densities could account for the magnitude and temperature dependences of the measured σ and Θ.

Figure 3 shows $\vec{b}$-axis conductivity for one sample for each of groups 2 and 3, and also indicates the conductivity measured in the directions $\vec{a}$ and $\vec{c}^*$ for typical group-3 samples. The latter is in-

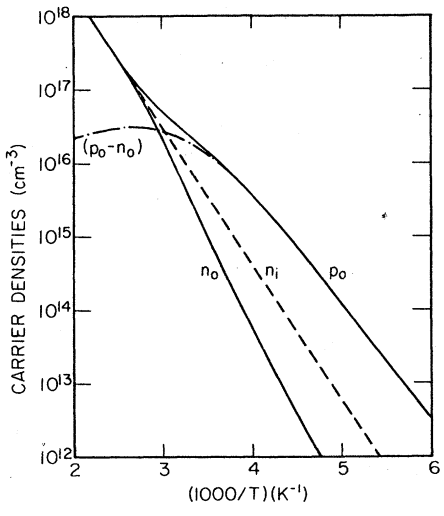

FIG. 6. Computed variation of carrier densities with $1/T$ for "intrinsic" $Cs_2(TCNQ)_3$ and for group-3 crystals. The curve for p_0-n_0 traces the course of $N_{ai}-N_d$; note that this decreases above about 370 K. A similar trend was computed also for group-2 material.

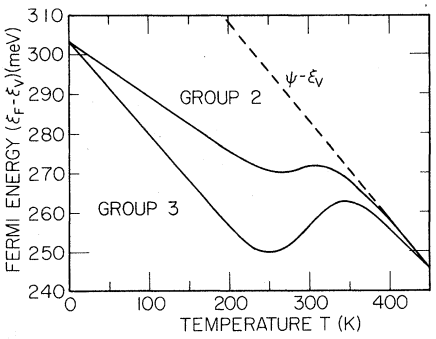

FIG. 7. Calculated Fermi energy vs T for group-2 and −3 crystals. In both cases, ϵ_F joins the intrinsic line of $\psi - \epsilon_v$ at high temperatures, and is asymptotic to $\epsilon_v + \epsilon_{a0}$ as $T \to 0$.

cluded merely to illustrate the size of the anisotropy factor separating conductivity along [010] from that in the (010) plane. The manner in which data points for 3*A* and 3*C** superimpose shows remarkably little anisotropy within that plane, as was further confirmed with Van der Pauw-type measurements. This is rather curious, since the directions $\vec{a}$ and $\vec{c}$* have such radically different thermopower characteristics.

Figure 4 shows how thermopower varies with temperature for six samples chosen as representative of many more that were measured; one for each of the directions $\vec{a}$, $\vec{b}$, and $\vec{c}$* for each of groups 2 and 3. The figure is complex, and confusing at first sight, but is necessary so that the various influences can be seen at work. At high temperatures, differences between groups 2 and 3 disappear, and one has "intrinsic" thermopower—positive for the $\vec{a}$ direction and negative for directions $\vec{b}$ and $\vec{c}$*. Room temperature lies at about the middle of a broad transition region in which thermopower is highly temperature-sensitive, and in which intersample differences are prominent. (The differences among several samples of a given group of crystals for a given orientation were much smaller than the differences shown here between groups 2 and 3; the six samples used for Fig. 4 were representative of the behavior of numerous crystals drawn from those two groups, the fruits of many hours of slow and patient measurements with fragile samples nurtured through successive temperature cycles.) And, finally, thermopower becomes large and positive for all samples of any crystal group or orientation at the lower end of the temperature range.

This last aspect of the thermopower was quite surprising, inasmuch as Siemons *et al.*[2] had reported a $\vec{b}$-axis thermopower that was negative at room temperature and became *more negative* on cooling (to $\simeq -1000$ μV/K at 200 K). It is our belief that the sample of Siemons *et al.* probably became n-type extrinsic on cooling, whereas all the material produced in this laboratory appears to become p-type extrinsic, with low-temperature properties controlled by partially compensated deep-level acceptor impurities.

The numerical analysis described in Sec. V indicates that these acceptor impurities have an ionization energy some 40% of the intrinsic gap width; it is the largeness of this impurity activation energy that makes the transition region for conductivity and especially for thermopower so broad. For comparison with results reported for another organic semiconductor, the impurity ionization energy found in the low temperature semiconducting phase of TTF-TCNQ from the photoconductive measurements of Eldridge[19] is some 30% of the total gap width.

The lines connecting data points in Figs. 3 and 4 are of two kinds. For the line connecting $\vec{a}$ and $\vec{c}$* direction conductivity data in Fig. 3, and for the lines connecting $\vec{a}$ and $\vec{c}$* thermopower data in Fig. 4, the lines do not represent any known equations; they simply indicate the trend of the points. However, the lines for $\vec{b}$-axis conductivity and thermopower samples in Figs. 3 and 4 (marked 2*B* and 3*B*) obey the equations discussed in the next section, with parameters found by computer fitting. The same $\vec{b}$-axis thermopower data for 2*B* and 3*B*, and the same computer-generated curves, is shown in Fig. 5 with reciprocal temperature as the abcissa, since that provides a more critical test of the quality of fitting.

V. DEEP-LEVEL ACCEPTOR MODEL

Soos and Klein[26] have developed a Hubbard-band model for $Cs_2(TCNQ)_3$ which takes into account the periodic disturbance of TCNQ spacings along the stack. Král and Khás[27] reached comparable conclusions, as did Bernstein.[42] The resulting 1D ($\vec{b}$-axis) model has Brillouin-zone boundaries at $\pm\pi/3b$, and three tight-binding bands. With no impurities, the lower band is full and the middle and upper bands empty. The widths of the lower (valence) and middle (conduction) bands and the width of the gap are determined by the ratio of site energy to charge-transfer integral.

In what follows, it is assumed (i) that the $Cs_2(TCNQ)_3$ bands are wide enough to validate the use of band concepts and of one-electron Fermi statistics, and (ii) that $\vec{b}$-axis motion resulting in an observed conductivity or Seebeck voltage can be accounted for in terms of a relaxation-time formalism. These assumptions are certainly open

to question, in view of the small carrier mobilities so deduced even for that favored direction. Motion within the (010) plane is almost certainly not describable in terms of Bloch functions.

During the process of computer modeling, an attempt was made at one stage to fit conductivity and thermopower data for all three directions as functions of temperature—using appropriately anisotropic mobilities. This attempt failed. After describing the model which does account for $\vec{b}$-axis data quite well, the rationale for temperature dependence of phenomena in directions $\vec{a}$ and $\vec{c}^*$ will be discussed.

In harmony with the model of Soos and Klein, we assume that both the valence and conduction bands have a tight-binding ($\sin^2$) form of dispersion. Let the valence band be of total width E_1, with ϵ_v as the upper energy limit; and let the conduction band be of width E_2, with $\epsilon_c = \epsilon_v + \epsilon_i$ as the lower edge. It may be expected that the intrinsic gap ϵ_i will vary with temperature, and the form $\epsilon_i = \epsilon_{i0} - \alpha T$ is the simplest and most natural assumption.

Since $Cs_2(TCNQ)_3$ is not a highly conducting material, it seems very safe to assume that the Fermi energy ϵ_F is well within the intrinsic gap. Thus Fermi integral forms for carrier densities simpli-by to their nondegenerate Boltzmann limits. The concentrations p_0 of valence band holes and n_0 of conduction band electrons then are given by

$$\begin{aligned} p_0 &= N_v \exp[-(\epsilon_F - \epsilon_v)/kT] , \\ n_0 &= N_c \exp[-(\epsilon_c - \epsilon_F)/kT] , \end{aligned} \tag{1}$$

where N_v and N_c are the effective densities of states in the valence and conduction bands respectively. For the 1D situation under consideration,

$$\begin{aligned} N_v &= (\zeta/V)(kT/\pi E_1)^{1/2} , \\ N_c &= (\zeta/V)(kT/\pi E_2)^{1/2} , \end{aligned} \tag{2}$$

where V is the unit cell volume, and the number ζ accounts for the statistical weight of the state with respect to the entire unit cell. For $Cs_2(TCNQ)_3$, $\zeta = 4$ and $\zeta/V = 2.40 \times 10^{21}$ cm^{-3}.

When impurities are of negligible effect, the intrinsic pair density is

$$n_i = (n_0 p_0)^{1/2} = (N_v N_c)^{1/2} e^{\alpha/2k} e^{-\epsilon_{i0}/2kT} \tag{3}$$

and the Fermi energy is at the intrinsic position

$$\begin{aligned} \psi &= \tfrac{1}{2}(\epsilon_v + \epsilon_c) + \tfrac{1}{2}kT \ln(N_v/N_c) \\ &= \tfrac{1}{2}(\epsilon_v + \epsilon_c) + \tfrac{1}{4}kT \ln(E_1/E_2) . \end{aligned} \tag{4}$$

However, we expect impurities to be important at all but the highest temperatures. For domination by acceptor impurities, such that the ratio $R = p_0/n_i = n_i/n_0 = (p_0/n_0)^{1/2}$ is greater than unity, then ϵ_F is lower than ψ:

$$\epsilon_F = \epsilon_v + kT \ln(N_v/p_0) = \psi - kT \ln R . \tag{5}$$

This affects the relative size of the contributions of holes and electrons to total conductivity and ambipolar Seebeck coefficient.

Let μ_p and $\mu_n = b\mu_p$ be the $\vec{b}$-axis mobilities of holes and electrons, respectively. Then the total conductivity is

$$\sigma = \sigma_p + \sigma_n = e\mu_p(p_0 + bn_0) , \tag{6}$$

which becomes $\sigma_i = en_i\mu_p(1+b)$ for the intrinsic situation of $p_0 \to n_i \to n_0$. The mixed conduction thermopower is

$$\Theta = (\sigma_n\Theta_n + \sigma_p\Theta_p)/(\sigma_n + \sigma_p) , \tag{7}$$

where the individual band Seebeck coefficients have the form

$$\begin{aligned} \Theta_p &= +(k/e)[A_p + (\epsilon_F - \epsilon_v)/kT] \\ &= +(k/e)[A_p + \ln(N_v/p_0)] , \\ \Theta_n &= -(k/e)[A_n + (\epsilon_c - \epsilon_F)/kT] \\ &= -(k/e)[A_n + \ln(N_c/n_0)] , \end{aligned} \tag{8}$$

in the relaxation-time (Boltzmann transport equation) approach. The numbers A_p and A_n are ratios of Γ functions, dependent on the energy dependence of scattering, and provide a measure of the excess energy transported by a mobile hole or electron (in excess of $\epsilon_F - \epsilon_v$ or $\epsilon_c - \epsilon_F$) as it diffuses along a temperature gradient. To cut a long story short, after many computer runs we conclude that the magnitude of thermopower in $Cs_2(TCNQ)_3$ can be properly related to the activation energies of conductivity only setting $A_p \simeq A_n \simeq 0$. This would be an astonishing assumption for an isotropic three-dimensional semiconductor, but it should be much less surprising for the present situation of 1D bands.

To complete the characterization of the model, assume that a crystal contains N_a monovalent acceptor impurities per cm^3, of which N_{ai} are ionized; and also a smaller density N_d cm^{-3} of fully ionized compensating donor impurities. Then neutrality requires that

$$p_0 = N_{ai} - N_d + n_0 . \tag{9}$$

Let the acceptor ground state energy be $\epsilon_a = \epsilon_{a0} - \gamma T$ above ϵ_v, and let the acceptor spin degeneracy factor be β. Then

$$N_{ai} = N_a(1 + p_0/p_1)^{-1} , \tag{10}$$

where the quantity p_1 (sometimes called the "mass-action constant") is given by

$$p_1 = (N_v/\beta e^{-\gamma/k}) \exp(-\epsilon_{a0}/kT) . \tag{11}$$

Our analysis has not provided an opportunity to determine values for acceptor state degeneracy β and acceptor energy temperature dependence γ separately; only for the quantity $\beta' = \beta e^{-\gamma/k}$. It has permitted us to deduce values for the quantities ϵ_{i0}, α, ϵ_{a0}, μ_p, and μ_n, along with values for N_a and N_d in crystals of groups 2 and 3.

In so doing, two further assumptions had to be made, and one variable was eliminated from consideration. In order to make the computation tractable, one assumption made was that each band be 0.25 eV in total width (not based on hard information, but not incompatible with optical spectra[30]), and the other assumption was that the *mobility ratio* $b = \mu_n/\mu_p$ not depend on temperature. Thus this requires that μ_p and μ_n share a common temperature dependence. What should that be? We have encouraged our computer to try modeling with a mobility that increases with temperature (as for impurity scattering, or for activated mobility), that varies as $T^{-3/2}$ (as with acoustical-phonon scattering), or that varies as T^{-n} with $3 < n < 4$ [as with the molecular phonon scattering invoked by Epstein *et al.*[12] in a recent conductivity analysis of N-methylphenazinium-TCNQ(NMP-TCNQ)]. To our surprise, the ability to fit the combination of conductivity and thermopower data over the entire temperature range is far superior when *temperature-independent* mobilities are used. The data is best fitted for a mobility ratio $b = \mu_n/\mu_p = 1.90$. Of course, this ratio must exceed unity for thermopower to be negative as $p_0 \rightarrow n_i \rightarrow n_0$.

Table I shows the complete set of parameters obtained by computer modeling with Eqs. (1)–(11), to simulate the conductivity and thermopower behavior for crystals of groups 2 and 3. The three parts of the table show the deduced intrinsic properties of the $Cs_2(TCNQ)_3$ lattice, the properties of the acceptors which appear to dominate the low-temperature behavior, and the concentrations necessary of these acceptors and of compensating donors for the observed temperature dependencies in these two groups of crystals. Some observations on the applicability of the model are made in Sec. VI.

TABLE I. Parameters derived from fitting experimental data.

(A) Intrinsic parameters	
ϵ_i	$(0.715 - 5.0\times10^{-4}T)$ eV
σ_i	$72T^{1/2}\exp(-0.358/kT)\ \Omega^{-1}\,\mathrm{cm}^{-1}$
n_i	$4.5\times10^{20}T^{1/2}\exp(-0.358/kT)\ \mathrm{cm}^{-3}$
$\mu_n = 1.90\mu_p$	$0.647\ \mathrm{cm}^2/\mathrm{V\,sec}$
(B) Acceptor properties	
ϵ_a	$0.303 - \gamma T$ eV
p_1	$6.3\times10^{19}T^{1/2}\exp(-0.303/kT)\ \mathrm{cm}^{-3}$
$\beta' = \beta e^{-\gamma/k}$	0.40
(C) Impurity concentrations	
Group-2 crystals: N_a	$7.53\times10^{16}\ \mathrm{cm}^{-3}$
N_d	$2.53\times10^{16}\ \mathrm{cm}^{-3}$
Group-3 crystals: N_a	$1.23\times10^{17}\ \mathrm{cm}^{-3}$
N_d	$1.77\times10^{16}\ \mathrm{cm}^{-3}$

VI. DISCUSSION

We believe that the essentials of the model sketched in Sec. V have a good probability of being correct. The actual numbers derived are obviously sensitive to the starting assumptions, to varying degrees. Most of the obvious changes in those starting assumptions have been tried with much poorer results. The evidence for intrinsic behavior at high temperatures is less strong than if it were possible to get thermopower data up to 500 K; but it is felt that the conductivity behavior at the higher temperatures, compared with optical data, makes an intrinsic identification plausible. Thus the values obtained for ϵ_i and $\alpha = -d\epsilon_i/dT$ are reasonable; $\epsilon_i \simeq 0.6$ eV at 300 K is in crude agreement with Hiroma's optical value,[30] and $\alpha = 5\times10^{-4}$ eV/K is quite typical of values found in other semiconductors.

The pre-exponential coefficient in the n_i expression is influenced both by α and by the bandwidths. Our formulation was weakened by setting $E_1 = E_2 = 0.25$ eV in order to reduce the number of variables to manageable proportion, and one hopes that the bandwidths in $Cs_2(TCNQ)_3$ will eventually be known. Since n_i varies as $(E_1E_2)^{-1/4}$, probably the coefficient of n_i, and the deduced carrier mobilities, are unlikely to be in error from this cause by a factor worse than 2. Thus, with some uncertainty, mobilities are a little less than 1 $\mathrm{cm}^2/\mathrm{V\,sec}$. This is just at about the minimum for which traditional transport models in a band are considered applicable.[43]

It was clear from the outset that the acceptor ionization energy ϵ_a would have to be large, since the temperature range of transition from apparently intrinsic to completely extrinsic conditions is so broad. Figure 6 shows the computed variation with $1/T$ of p_0, n_0, n_i, and $p_0 - n_0 \equiv N_{ai} - N_d$ for material of group-3 crystals. Group 3 is used for illustration here since it has the largest N_a and smallest N_d/N_a; the compensation is still quite appreciable. Compensation has to be expected, (i) in view of the variety of native and foreign de-

fects which might have some opportunity for incorporation in a growing crystal from solution, and (ii) in view of the n-type behavior (negative thermopower) reported by Siemons *et al.*[2] Their crystal may well have contained an excess of deep donors over acceptors, whereas ours invariably seem to contain more acceptors than donors. We have attempted to change conditions (in preparations other than just groups 1–3) to produce n-type behavior, but have not succeeded.

The values for N_a and N_d in Table I amount to no more than 0.01% of the TCNQ sites, and one may expect that other (non-electrically-active) impurities are also present. The size of ϵ_a makes it hard for the acceptors to seize control as temperature is reduced, and study of the resulting Fermi energy ϵ_F demonstrates this. Figure 7 shows ϵ_F vs T as calculated for both groups 2 and 3; partial compensation requires that ϵ_F be asymptotic to $\epsilon_v + \epsilon_{a0}$ as $T \to 0$. Rising temperature causes partial ionization of the acceptors and a fall in ϵ_F, a trend reversed as N_{ai} is no longer able to increase. Finally, ϵ_F is forced down again to join the falling intrinsic line. It is interesting to observe that, in contrast to a shallow-impurity situation, here the acceptors never achieve full ionization; the onset of intrinsic conduction forces ϵ_F downwards and obliges N_{ai} to *decrease* at the highest temperatures. That can be seen in the curve of $p_0 - n_0 = N_{ai} - N_d$ towards the left of Fig. 6.

The numerical analysis was unable to predict β and γ separately, but did yield $\beta' = \beta e^{-\gamma/k} = 0.40$. Note that if ϵ_a/ϵ_i is invariant with T, then $\gamma = \alpha\epsilon_{a0}/\epsilon_{i0} \simeq 2 \times 10^{-4}$ eV/K, for $\beta = \beta' e^{\gamma/k} \simeq 5$; a quite reasonable number for the spin degeneracy factor of an acceptor impurity.

Thus the model, while not proved, is rather satisfactory in its description of what controls carrier densities in $Cs_2(TCNQ)_3$, and how this determines $\vec{b}$-axis σ and Θ. Unanswered questions include (i) the nature of active acceptor and donor impurities, and (ii) why apparent mobilities should be temperature-independent. The smallness of mobility compared with that in NMP-TCNQ (see Ref. 12) is not surprising, since that solid benefits from conduction along a uniform TCNQ stack, with optimum opportunities for π overlap.

Band motion in $Cs_2(TCNQ)_3$ is indicated only for the stacking direction. This suggests bandlike wave functions along [010], decaying in transverse directions. Finite overlap is possible between wave functions on adjacent stacks, but transport in the (010) plane is apt to be hopping in nature. This should be inherently anisotropic within (010), for n- and p-type wave functions will not necessarily overlap to the same extent in the various transverse directions. Apropos the significance of this for thermopower in transverse directions, Cutler and Mott[44] and Fritzsche[45] have related carrier energy, conductivity and Seebeck effect by

$$\sigma\Theta = -\int \frac{\epsilon - \epsilon_F}{eT}\,\sigma(\epsilon)\,d\epsilon\,, \tag{12}$$

which does not involve mobility explicitly. Then sign and magnitude of Θ can be discussed without reference to a mobility ratio, and activated hopping can be accommodated as well as band motion. Thus transverse coefficients of Θ in $Cs_2(TCNQ)_3$ can plausibly reflect the statistical behavior of p_0 and n_0 as deduced from $\vec{b}$-axis properties; when ϵ_F is controlled at low temperatures by p-type extrinsic influences, thermopower will be positive for all directions. That is, of course, what is seen in Fig. 4. Under high-temperature intrinsic conditions, the differences in sign of Seebeck components for directions $\vec{a}$ and $\vec{c}^*$ may be judged as arising from differences in hopping opportunities for those two directions.

ACKNOWLEDGMENTS

We wish to acknowledge the support of this work by NSF through Grant No. DMR74-24208. Additionally, we wish to thank Dr. A. Lombardo for preparation of the crystals used in this work, and Dr. M. J. Schneider for advice on the crystallography of $Cs_2(TCNQ)_3$. Additional helpful discussions which we should like to acknowledge were held with Dr. U. Bernstein, Dr. P. M. Chaikin, Dr. A. J. Epstein, Dr. J. B. McGuire, Dr. Z. G. Soos, and Dr. J. B. Torrance.

*Present address: Oregon Graduate Center, Beaverton, Ore. 97005.
†Present address: University of Tennessee, Knoxville, Tenn. 37916.
‡Present address: Rice University, Houston, Tex. 77001.

[1]R. G. Kepler, P. E. Bierstedt, and R. E. Merrifield, Phys. Rev. Lett. 5, 503 (1960).
[2]W. J. Siemons, P. E. Bierstedt, and R. G. Kepler, J. Chem. Phys. 39, 3523 (1963).
[3]I. F. Shchegolev, Phys. Status Solidi A 12, 9 (1972).
[4]*Chemistry and Physics of One-Dimensional Metals*, edited by H. J. Keller (Plenum, New York, 1977).
[5]*Highly Conducting Organic Materials*, edited by F. Wudl (Academic, New York, to be published).
[6]J. Ferraris, D. O. Cowan, V. Walatka, and J. H.

Perlstein, J. Am. Chem. Soc. 95, 948 (1973).
[7]L. B. Coleman, M. J. Cohen, D. J. Sandman, F. G. Yamagishi, A. F. Garito, and A. J. Heeger, Solid State Commun. 12, 1125 (1973).
[8]*Organic Conductors and Semiconductors*, edited by L. Pal (Springer, Berlin, 1977).
[9]Z. G. Soos, Ann. Rev. Phys. Chem. 25, 121 (1974).
[10]G. D. Stucky, A. J. Schultz, and J. M. Williams, Ann. Rev. Mater. Sci. 7, 301 (1977).
[11]J. Kommandeur, in *Low-Dimensional Cooperative Phenomena*, edited by H. J. Keller (Plenum, New York, 1975), p. 65.
[12]A. J. Epstein, E. M. Conwell, D. J. Sandman, and J. S. Miller, Solid State Commun. 23, 335 (1977).
[13]D. Kuse and H. R. Zeller, Phys. Rev. Lett. 27, 1060 (1971).
[14]M. J. Rice and J. Bernasconi, J. Phys. F 3, 55 (1973).
[15]J. P. Farges, Phys. Lett. A 43, 161 (1973).
[16]A. Brau and J. P. Farges, Phys. Status Solidi B 61, 257 (1974).
[17]L. I. Buravov, D. N. Fedutin, and I. F. Shchegolev, Sov. Phys. JETP 32, 612 (1971).
[18]P. M. Chaikin, J. F. Kwak, T. E. Jones, A. F. Garito, and A. J. Heeger, Phys. Rev. Lett. 31, 601 (1973).
[19]J. E. Eldridge, Solid State Commun. 21, 737 (1977).
[20]C. K. Chiang, C. R. Fincher, Y. W. Park, A. J. Heeger, H. Shirakawa, E. J. Louis, S. C. Gau, and A. J. MacDiarmid, Phys. Rev. Lett. 39, 1098 (1977).
[21]D. B. Chesnut and P. Arthur, J. Chem. Phys. 36, 2969 (1962).
[22]P. Arthur, Acta Crystallogr. 17, 1176 (1964).
[23]C. J. Fritchie and P. Arthur, Acta Crystallogr. 21, 139 (1966).
[24]S. F. Lin, W. E. Spicer, and B. H. Schechtman, Phys. Rev. B 12, 4184 (1975).
[25]J. B. Torrance and B. D. Silverman, Phys. Rev. B 15, 788 (1977).
[26]Z. G. Soos and D. J. Klein, J. Chem. Phys. 55, 3284 (1971).
[27]K. Král and Z. Khás, Czech. J. Phys. B 24, 914 (1974).
[28]J. S. Blakemore, U. Bernstein, J. E. Lane, and D. A. Woodbury, *Proceedings of the Thirteenth International Conference on the Physics of Semiconductors, Rome*, 1976, edited by F. G. Fumi (Academic, New York, 1977), p. 345.
[29]Y. Iida, Bull. Chem. Soc. Jpn. 42, 637 (1969).
[30]S. Hiroma, H. Kuroda, and H. Akamatu, Bull. Chem. Soc. Jpn. 44, 9 (1971).
[31]R. M. Vlasova, A. I. Gutman, L. D. Rozenshtein, and N. F. Kartenko, Phys. Stat. Solidi B 47, 435 (1971).
[32]J. B. Torrance, B. S. Scott, and F. B. Kaufman, Solid State Commun. 17, 1369 (1975).
[33]N. Sakai, I. Shirotani, and S. Minomura, Bull. Chem. Soc. Jpn. 45, 3314 (1972).
[34]L. R. Malby, R. J. Harder, W. R. Hertler, W. Mahler, R. E. Benson, and W. E. Mochel, J. Am. Chem. Soc. 84, 3374 (1962).
[35]From Aldrich Chemical Company, and from K & K Laboratories.
[36]Provided through the courtesy of Lithium Corporation of America.
[37]Groups 1 and 2 in this paper correspond to crystal batches 12 and 13 of Ref. 28.
[38]L. J. van der Pauw, Philips Res. Rep. 13, 1 (1958); 16, 187 (1961).
[39]H. C. Montgomery, J. Appl. Phys. 42, 2971 (1971).
[40]W. L. V. Price, J. Phys. D 5, 1127 (1972).
[41]P. M. Chaikin and J. F. Kwak, Rev. Sci. Instrum. 46, 218 (1975).
[42]U. Bernstein (unpublished calculation made available to us).
[43]The lower limits of mobility were discussed by H. Fröhlich and G. L. Sewell, Proc. Phys. Soc. London 74, 643 (1959); and the topic is discussed by A. F. Ioffe, *Physics of Semiconductors* (Academic, New York, 1960), p. 180.
[44]M. Cutler and N. F. Mott, Phys. Rev. 181, 1336 (1969).
[45]H. Fritzsche, Solid State Commun. 9, 1813 (1971).